each polishing step, to minimize the cold work in the surface. An optically flat, mirrorlike surface was finally achieved by polishing on a silk cloth impregnated with fine alumina powder.

The samples were then annealed at 380 °C in vacuum for at least five days, to remove any lattice strains that might have resulted from polishing. Those samples that showed any signs of recrystallization were rejected immediately. Furthermore, a back-reflection x-ray photograph of each specimen was taken to determine the extent of residual lattice strain as well as crystallographic orientation. Only those samples that were strain free and had their principal axes to within 15° of the cylindrical axis were used for diffusion anneals.

The flat end of each specimen was then electroplated with Zn^{65} from a standard cyanide solution.[21] The thickness of the radioactive layer was estimated to be of the order of 100 atomic layers.

B. Procedure

As D_b depends on a weighted difference of D_a and D_c, the principal-axis diffusion coefficients were obtained in pairs by annealing a- and c-axis single-crystal specimens simultaneously. The weighted difference is then less subject to errors arising from uncertainties in the temperature and pressure than would be the case if D_a and D_c were obtained separately.

The a- and c-axis samples were wrapped in a molybdenum[22] foil with their active faces separated by a thin molybdenum disk. They were placed in a pressure vessel which was subsequently pressurized and then submerged in a well-stirred molten-tin bath whose temperature could be controlled and reproduced to ±0.2 °C. A detailed description of the apparatus, including the pressure vessel and the molten-tin bath, is given elsewhere.[23]

For a particular isotherm, the diffusion anneals were run for the same duration, as it was found that the warm-up time was independent of the pressure. Thus, warmup corrections, although affecting the absolute value of the diffusion coefficients by only a few percent, have no effect on the quantity $(\partial \ln D/\partial p)_T$ and hence on the activation volume ΔV.

After the specimens were run for a time appropriate to obtain a penetration depth of ~50 μ, the self-diffusion coefficients were obtained by the usual radiotracer lathe-sectioning techniques.[24]

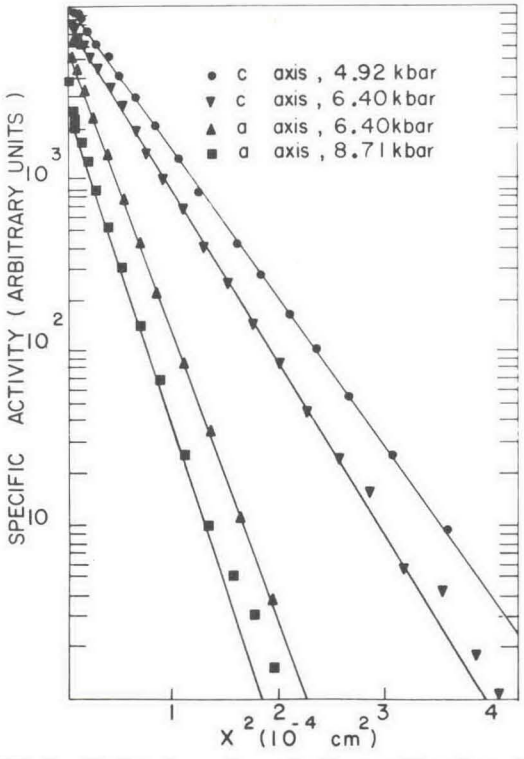

FIG. 1. Best and worst penetration profiles for self-diffusion in zinc at 350.7 °C.

IV. EXPERIMENTAL RESULTS

A. Penetration Profiles

Typical penetration profiles for self-diffusion in zinc at 350.7 °C are shown in Fig. 1. It is quite evident that they are Gaussian over at least $2\frac{1}{2}$ orders of magnitude in tracer specific activity. However, some of these penetration profiles do exhibit a tail, indicative of short circuiting at deep penetration distances. In such cases, the bulk diffusion coefficient was determined by considering only the linear segment of the penetration profile, ignoring the tail. The principal-axis self-diffusion coefficients $D_c(T, P)$ and $D_a(T, P)$ are listed in Table I.

B. Isotherms

The variation of $\ln D_c$, $\ln D_a$, and $\ln D_b$ with pressure at temperatures of 400.8, 350.7, and 300.9 °C are shown in Fig. 2. These isotherms are obviously linear over a pressure range of 0 to 9 kbar. The zero-pressure data of Peterson and Rothman[10] and Batra[11] are in excellent agreement with the present data, while those of Shirn *et al.*[9] do not agree nearly as well. More significantly, the zero-pressure data of the present experiment taken in the same way as those of the high-pressure runs, are obviously consistent with the rest of the present data.

Least-squares-fit lines were used to obtain the slopes of these isotherms and hence the activation volumes ΔV_c and ΔV_b in accordance with Eqs. (1) and (2). The $\kappa_c \gamma_c$ term in Eq. (1) is of the order of 3% of the first term and cannot be ignored, as

TABLE I. Self-diffusion coefficients for zinc.

p (kbar)	T (°C)	D_c (10^{-9} cm^2/sec)	D_a (10^{-9} cm^2/sec)
0.131	400.8	9.449	5.846
1.938	400.8	8.381	5.174
3.495	400.8	7.300	...[a]
3.895	400.8	7.133	4.503
5.107	400.8	...[a]	4.135
6.863	400.8	5.812	3.586
7.028	400.8	5.792	3.574
8.910	400.8	4.872	2.963
0.133	350.7	2.550	1.505
1.380	350.7	2.286	1.360
1.860	350.7	2.200	...[b]
3.380	350.7	1.968	1.146
4.920	350.7	1.750	...[b]
4.990	350.7	...[b]	1.047
6.400	350.7	1.580	0.933
8.710	350.7	1.345	0.789
0.100	300.9	0.5443	0.2953
0.913	300.9	0.5119	0.2746
1.916	300.9	0.4728	0.2542
5.093	300.9	0.3696	0.2032
6.564	300.9	0.3340	0.1779
8.349	300.9	0.2907	0.1579

[a]Samples recrystallized during run.
[b]Samples destroyed while sectioning.

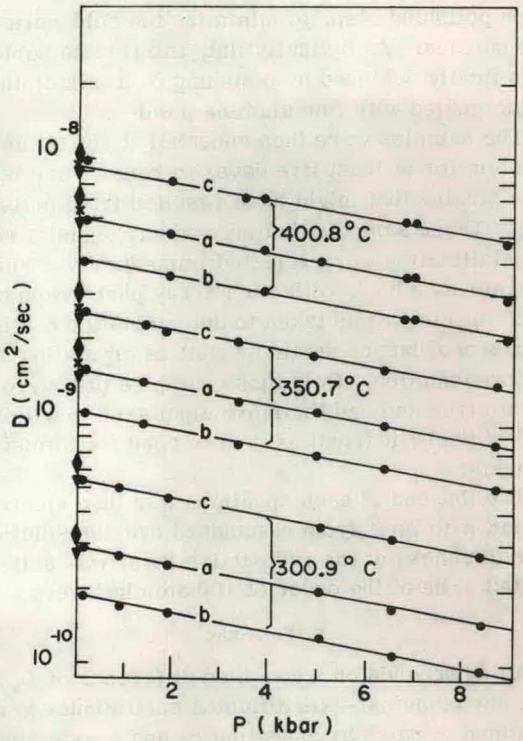

FIG. 2. Isotherms of $\ln D_c$, $\ln D_a$, $\ln D_b$ vs p for temperatures of 400.8, 350.7, and 300.9 °C. The ♦, ▼, and ×, are data from Refs. 9–11, respectively.

the activation volumes are measured to the unusually high precision of a few percent. On the other hand, in Eq. (2) the $\kappa_a\gamma_a$ term is only of the order of 0.3% of the first term, and therefore makes a negligible contribution. The values of the linear compressibilities and Grüneisen constants were obtained from the data of Alers and Neighbors[25] and Grüneisen and Goens,[26] respectively. The activation volumes $\Delta V_c(T)$ and $\Delta V_b(T)$ are given in Table II.

C. Variation of Activation Volume with Temperature

The activation volumes ΔV_c and ΔV_b, listed in Table II, show a systematic linear decrease with decreasing temperature. This dependence is a result of the constancy of the terms $(\partial \ln D_c/\partial p)_T$ and $[\partial \ln(D_a - gD_c)/\partial p]_T$, which then become proportionality factors between ΔV and T in Eqs. (1) and (2).

Also, as can be seen from Table II, the slopes of the isotherms and hence the basal and nonbasal activation volumes at a particular temperature are equal to within the experimental uncertainty. Thus in Fig. 3, both ΔV_b and ΔV_c have the same variation with temperature. A linear least-squares fit to the six data points of ΔV vs T gives

$$\left(\frac{\partial \Delta V}{\partial T}\right)_p = (6.4 \pm 0.5) \times 10^{-3} \text{ cm}^3/\text{mole}^\circ\text{K}.$$

D. Variation of Activation Enthalpy and Entropy with Pressure

Arrhenius plots of $\ln D_c$ vs $1/T$ and $\ln D_b$ vs $1/T$ at pressures of 0.10, 1.92, 5.00, and 8.88 kbar are given in Figs. 4 and 5, respectively. By choosing these pressures, the chosen experimentally measured diffusion coefficients for a particular isobar were corrected by no more than 2% in being

TABLE II. Isotherm slopes and activation volumes in zinc.

T (°C)	$-\left(\frac{\partial \ln D_c}{\partial p}\right)_T$ (kbar)$^{-1}$	$-\left(\frac{\partial \ln (D_a - gD_c)}{\partial p}\right)_T$ (kbar)$^{-1}$	ΔV_c (cm^3/mole)	ΔV_b (cm^3/mole)
400.8	0.074 029 ± 0.0015	0.076 718 ± 0.0024	4.28 ± 0.08	4.30 ± 0.14
350.7	0.073 953 ± 0.0010	0.074 666 ± 0.0015	3.97 ± 0.05	3.92 ± 0.09
300.9	0.076 061 ± 0.0006	0.075 345 ± 0.0017	3.72 ± 0.03	3.59 ± 0.09